

## **A SELF-ADJUSTABLE STEP-BASED CONTROL ALGORITHM FOR A GRID-INTERACTIVE MULTIFUNCTIONAL SINGLE-PHASE PV BATTERY SYSTEM UNDER ABNORMAL GRID CONDITIONS**

**S.Selvakumar Raja** Principal & Professor, ECE Department, Kakatiya Institute of technology and science for women, Nizamabad, Telangana, India, Email: kitswnzb@gmail.com

**B.Mahendar** Associate Professor & HOD, EEE department, Kakatiya Institute of technology and science for women, Nizamabad, Telangana, India, Email: kitswnzb@gmail.com

### **ABSTRACT**

This article describes a power grid-compatible, single-phase photovoltaic (PV) system that can transmit power with ease. Utilities benefit from improved power quality because to this versatile PV-battery combination. Nonlinear loads will continue to get electricity from the system regardless of the availability of green energy sources and utilities. In order to set up PV batteries, you need two things. The dc-link is equipped with a bidirectional converter and a PV array boost converter, allowing it to store energy in batteries, forming the initial stage. The voltage source converter (VSC) compensates for reactive power, filters out harmonics, and feeds surplus energy back into the grid. When working independently, the islanded method guarantees that the voltage of the load stays sinusoidal. A proportional integral controller can sustain a consistent dc-link voltage. A feed-forward control is used in order to increase the responsiveness of the PV-battery system to variations in load, solar PV integration is necessary. This inquiry enhances the VSC with an independent step-based control. To demonstrate the operation of the PV-battery system, it is assumed that the actual power is equivalent to the load current. Research that makes use of simulations makes use of the MATLAB Simulink application. The PV-battery combination has proven to be sufficiently effective in testing, withstanding significant grid stress. Power quality, PV, sag, surge, VSC, and MPPT are all significant terms.

**Index Terms**—MPPT, power quality, PV, sag, swell, VSC.

### **I INTRODUCTION**

As PV-battery systems become more cost-competitive with grid electricity, their popularity rises. Grid-connected solar systems must be deactivated during a distribution network outage for safety purposes. A utility interactive PV system with energy storage is a great choice for providing continuous energy during emergencies while also managing peak power usage. Battery storage can help reduce the effects of intermittent PV generation when this situation occurs. A bidirectional power converter is required to regulate the negative and positive aspects of the battery storage simultaneously. A solar cell's efficiency in converting solar radiation into usable energy is sensitive to temperature and irradiance. The voltage-current curve of the solar array is not constant and might alter in certain cases. One must locate a singularity on the power versus voltage curve in order to maximize energy extraction from a PV grid.

The operating point is sensitive to changes depending on meteorological circumstances. The investigators analyzed different approaches for monitoring the maximum power point. We analyzed MPPT controllers designed for grid-connected PV arrays. The perturb and observe MPPT method

with an adjustable step size is utilized in standalone PV systems. An MPPT approach based on change in conductance is introduced. This article uses the incremental conductance method because of its simple implementation and positive results in dealing with changing levels of sunlight. Grid-connected VSCs are widely used in several fields. Various VSC-based system configurations connected to the grid are depicted. Scholars demonstrate the use of VSC and distribution strategies in constructing active power filters. D-STATCOMs provide current through an inductor situated at the point of common coupling. The VSC can operate by applying a precise voltage across a dc-link capacitor. The VSC is commonly seen as a shunt-connected device in several situations. The D-STATCOM supports many control algorithms. Comprehensive compensations are offered for VSC current control in wind farms operating on a weak grid, based on the current inaccuracy. A second-order generalized integrator control approach is proposed.

Several studies have shown that the grid-connected PV battery system has additional roles than providing electricity to the grid. The functions consist of dc link voltage management and reactive power adjustment. The solar PV-battery system connected to the grid includes a DSTATCOM feature and employs a fuzzy-PI controller to regulate the dc-link voltage and offset reactive power. This text discusses the use of a lattice wave digital filter to reduce harmonics in a grid-connected solar photovoltaic system. The system is a grid-connected, three-phase, single-stage photovoltaic battery system with precise quadrature control. The diagram shows the smooth shift from standalone to grid-connected modes of a utility interactive single-phase photovoltaic battery system. The power quality parameters of several grid converter topologies are shown. To alleviate the load-induced pressure on the PI controller caused by overshoot in the dc-link voltage, load compensation is applied using the feed-forward term. The literature on a digital filter-based active filtering system is discussed. Active power filters are shown to use adaptive harmonic detection with adjustable step size. Self-adjustable step control is used to operate a utility-connected PV battery system in this study.

The control approach generates distinct estimates for PV power participation, losses, and load current. Feed forward control reduces the load on a PI controller by adjusting for power fluctuations from a photovoltaic array and managing the variability of sunlight levels. This inquiry involves imperfect grid conditions. Various grid characteristics, capacity fluctuations, and weather conditions lead to a wide range of consequences. The PV-battery system's performance was considered satisfactory in this study. As per IEEE 1547, A grid-interactive PV battery system must produce a constant, sinusoidal AC voltage that is compatible with the utility grid's frequency and voltage in order for solar electricity to be fed into the grid.

A compact, reliable, and accurate synchronization mechanism is essential. Inefficient synchronization techniques can lead to instability, damage to important loads, and potential disruption of the distribution network. PLLs have been used for many years to synchronize VSCs with the power grid because of their endurance and monitoring features. The SRF-PLL is highly dependable and can quickly identify the phase angle when the system is sinusoidal. Although the input signal may include harmonics and be very variable, these methods significantly increase the variance of the recovered signal. The PLL improves efficiency under distorted situations by using an in-loop filter or a pre-filter.

Single-phase SRF-PLL is highly sensitive to harmonics and grid voltage synchronization under conditions of under voltage distortion, affecting the anticipated phase and frequency of the distribution network. This study utilizes a control strategy that relies on third-order sinusoidal integrators (SSIs) to reduce dc offset errors and assess the distribution network's ability to adjust to changes in angle and frequency. By employing a variable learning control and a third-order SSI-based approach, the PLL's natural capacity to resist shocks is improved. The interactive grid system stays functional even after a grid outage. Hence, a simple and effective approach for identifying

islanding is required to desynchronize the system from the grid in case of a malfunction. Many academic studies have raised issues regarding islanding detection. Scholars have recently studied communication-based islanding, hybrid techniques, including active and passive methodologies. Each of these strategies has its own set of pros and cons. Communication-based solutions cover a larger part of the nondetection zone (NDZ), but they are more expensive due to the requirement of additional communication equipment. Passive islanding has a greater non-detection zone (NDZ) compared to communication islanding and does not need any communication equipment. Because the article has a low NDZ and system rating, island detection does not require an extra communication device.

A direct passive islanding detection approach is constructed, relying on observations of grid voltage magnitude, phase, and frequency. The following are the results and advantages of the PV-battery microgrid: In this situation, islanding is detected utilizing a simple and seamless passive detection method that relies on monitoring the voltage, angle, and frequency of the grid. No extra communication equipment is required. Low operating costs and simple transfer protect loads from critical problems during load changes. The PLL is prone to disturbances and noise, leading to reduced tracking accuracy in complex and changing environments. However, the system maintains stability even when grid conditions fluctuate due to factors like distribution network changes and contaminated utility scenarios. The third-order SSI-based approach, in combination with mode transfer control, addresses the limitations of the traditional PLL. PLL does not decide either the dual loop frequency or the synchronization signals. Fluctuations in input grid voltages result in the PLL performing less effectively compared to the third-order SSI. Third-order SSI control maintains stable even with minor loop increases because of its dual loops.

When in utility interactive mode, the dc-ac converter acts as a compensator unit, decreasing the frequency of higher order harmonics generated by the load and supplying the necessary reactive power. During a grid outage, an islanding algorithm is used to maintain the load voltage structure and efficiently provide energy to loads. After switching from grid-interactive to standalone mode, the control algorithms are reconnected smoothly without causing instability or disturbance in the output voltage. Operating with a nonlinear imbalanced load is challenging because to the fluctuating frequency and voltage, which helps protect residential loads.

## II SYSTEM STRUCTURE

It is a method of generating energy by converting light into electrical current. Solar power systems and PV structures are other names for it produces usable solar electricity using photovoltaic processes. Solar-powered sheets are used to convert DC electricity to AC electricity in reaction to sunlight, along with a sun-controlled inverter for the conversion process. Additional equipment is needed for mounting, wiring, and system design. To address the rising costs of limit devices, the design might include a solar-powered backup system to improve its operation and enable seamless connection with a planned battery system. A sun-facing display typically consists just of sun-controlled panels, which form the basis of the photovoltaic system. The extra gear, often as dense as a building on top (BOS), is not included. Photovoltaic systems Contrast this with technologies like concentrated solar power or solar-based heat, which can be utilized for both heating and cooling; they convert light into energy quite effectively.

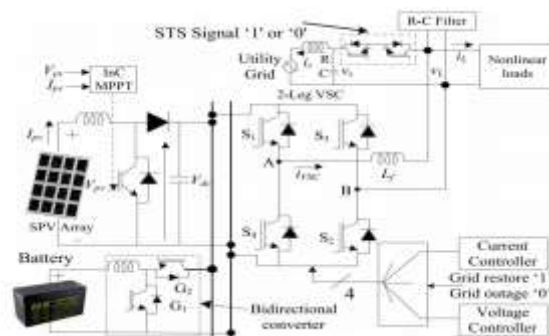


Fig. 1 An interactive grid system based on photovoltaic batteries

Figure 1 depicts the grid-interactive, multifunction PV battery system. This system consists of four fundamental elements. Parts that make up the SECS mainly include a VSC and an AC two-phase boost converter. A battery storage device with a bidirectional switch is the second option. The load-linked third component is the single-phase distribution grid, which is the fourth main component. It consists of a ripple filter and an interacting inductor. The 4 kW photovoltaic array consists of PV panels coupled in parallel and series. A boost converter uses MPPT control to maximize the output from a solar array. To power the DC link of the VSC, the boost converter must be used. The power quality of the single-phase utility network is improved when solar PV energy is transferred to the grid using the PV-battery system's Voltage Source Converter (VSC). A full-bridge Voltage Source Converter (VSC) with four IGBT switches and an interface inductance is coupled to the single-phase unit. A reduction in voltage switching pulses can be achieved by connecting an R-C filter to the PCC. During peak demand periods, the distribution network is fortified by utilizing battery storage technology, which reduces power fluctuations from the PV array. It provides the necessary energy in the event of a disaster when the PV array isn't producing power due to a power outage in the grid. The stacking of static transfer switches allows for the transfer of electricity to and from the power grid. The main grid regulates the operation of these switches.

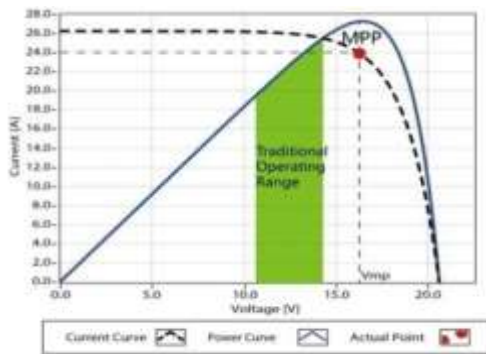
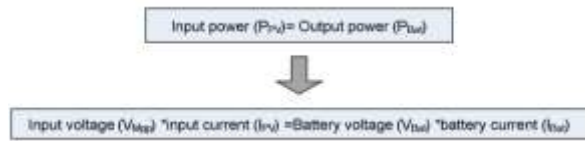
#### A. MPPT

This regulator utilizes MPPT computing to efficiently and precisely track the MPP of a solar array, maximizing solar energy gathering. This leads to a notable increase in production within the nearby planetary system. There are two possible methods for the presentation task: 1) Using an LCD display nearby, and 2) Utilizing an LCD meter placed at a fixed distance. Moreover, the regulator includes a Modbus communication protocol interface, which facilitates the integration of additional tests across many applications. Advanced electronic safety features and thorough self-assessment mechanisms make the solar charge regulator safe for users and minimize the chances of system component damage caused by configuration errors or malfunctions.

Especially noteworthy are: Superior components outperform Advanced MPPT technology by 99.5%. The framework demonstrates outstanding performance with a maximum transformation efficiency of 98%, ultra-optimized speed, and guaranteed productivity after upgrades. Reliability detects and monitors many points of maximum force. The programmable restriction on the maximum potential PV input power ensures that a wide range of operations will not be overburdened. Discharge Voltage of MPP Identification of adjustable framework voltages set at 12V and 24V DC.

The LCD display conveys information and operational status clearly and vividly without being explicitly stated. Various accumulation control modes are available, such as test, manual, On/Off, and On + Timer, along with client-defined charging restrictions for gel, sealed, and flooded batteries. Thermal management for battery performance optimization Use real-time energy assessment data. External LCD display (MT50, optional) connection and Modbus communication

protocol with RS-485 communication interface for PC network to set and monitor two boundaries. Updates to firmware.



(a)

(b)

Fig.2 Maximum Power Point Curve

In Figure 2 shows the maximum force point bend of a solar-powered board when obstructed by clouds, trees, snow, and other objects. The variation in charging range between two prevalent PWM regulators is dictated by the hidden area.

### III CONTROL APPROACHES

Control strategies determine the operational processes of a PV-battery system. The control strategies include an islanded algorithm, a battery controlled by a DC-DC converter that works in both directions, a synchronizing driver with a passive islanding detection technique to switch step-by-step voltage control mode and a distinct approach to system management in current control mode. Figure 3 demonstrates the present control method. The following characteristics are evaluated: Presently, instantaneous current ( $i_g$ ), photovoltaic  $V_{pv}$ , direct  $V_{dc}$ ,  $i_L$ , and  $v_g$ . Six feedback and control aspects have been discovered as a result. This generic control approach comprises two main portions. The primary focus is in order to make the MPPT function work more smoothly, boost converter control modifies the duty cycle of a boost converter. The dc-link of the VSC transmits the maximum power that a solar PV system is capable of producing to the electrical grid.

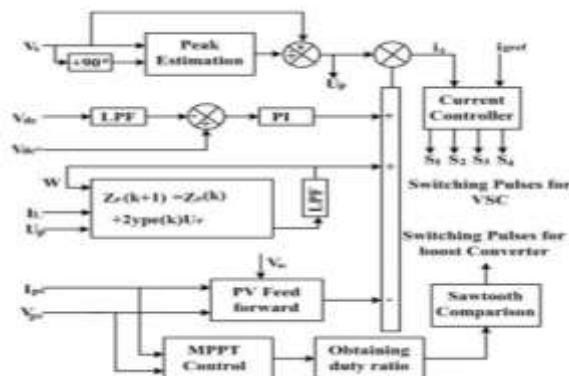


Fig. 3 VSC regulation in a grid-connected setup

The approach is considered multifunctional since it enhances the power output from the single-phase system to the grid simultaneously without sacrificing quality. The current found in the

grid maintains a unity power factor (UPF) and sinusoidal waveform consistently, irrespective of demand. The VSC provides the load with reactive and harmonic currents based on the instructions of the newly designed control algorithm. The duty cycle of the battery converter is evaluated under various charging and discharging conditions.

**A. Configuring VSC controls for interactivity with a grid:**

The VSC, as part of the SECS, is responsible for injecting Controlling reactive power, blocking current harmonics, and increasing the power factor to 1 are all achieved by incorporating solar PV power into the system. These objectives have been accomplished by the present of VSC. The new method of control relies on synchronizing the actual power output of the various PCC components. Here you may find a detailed description of the method for independently Step-based control that can be changed. In order to obtain the up alignment signal, the PCC voltage is utilized. Since the synchronization signal's phase and magnitude are identical to those of the PCC voltage, we may say that it is a sine wave. You have to make a prediction about where the PCC voltage will go up in order to obtain the synchronization template, which is provided by

$$V_p = \sqrt{v_\alpha^2 + v_\beta^2} \tag{1}$$

$V_p$  indicates the peak voltage at PCC,  $v_\beta$  represents the grid voltage, and  $v_\alpha$  represents the advanced grid voltage at a 90° phase. The synchronization signal is calculated using the peak value of the PCC voltage.

$$u_p = v_\alpha / V_p \tag{2}$$

The maximum load current is determined using a step-based self-adjusting control. The implemented control utilizes a single neuron. The controlling formula is:

$$Z_p(k+1) = Z_p(k) + 2\gamma_p e(k) u_p \tag{3}$$

The learning rate ( $\gamma_p$ ) of phase neurons is assessed. It is feasible to modify the learning rate of neurons in this phase. The equations needed to sustain the variable learning rate are as follows:

$$\gamma_p(k) = \varepsilon \left( 1 - \exp \left\{ 1 - \rho |x(k)|^2 \right\} \right) \tag{4}$$

$$x(k) = \tau x(k-1) + (1 - \tau) \{ e(k) - e(k-1) \}. \tag{5}$$

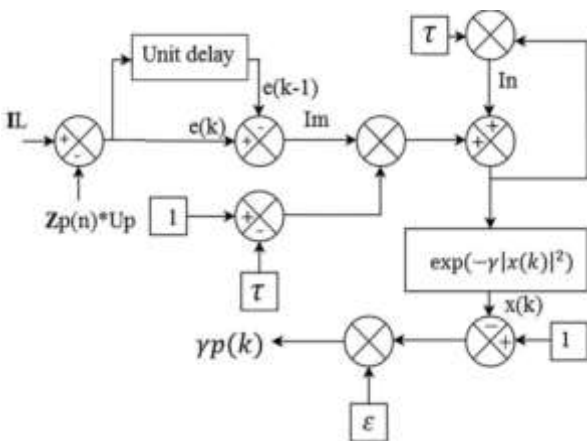


Fig.4 Four-step, self-regulating control for extracting peak load current

The difference between the measured and anticipated values is represented by  $e(k)$  and  $e(k - 1)$ . The values chosen for  $\varepsilon$ ,  $\rho$ , and  $\tau$  are 0.55, 0.45, and 0.8, respectively, as indicated in reference [24]. The comprehensive algorithm is currently in operation, as shown in Figure 4. The value of  $\gamma_p$  depends on the load current. Combining PV power participation to generate grid current results in the following outcome:

$$I_{pvff} = I_{pvq} = 2P_{pv} / V_p \tag{6}$$

$I_{pv}$  is the maximum grid current value in a lossless system where the load is compensated, resulting in no real power consumption. The PI controller has stabilized the dc-link voltage. The PI controller's output, computed as the loss component of the VSC, is

$$I_{loss}(n) = I_{loss}(n-1) + K_p \{V_{dc}(n) - V_{dc}(n-1)\} + K_i V_{dc}(n). \quad (7)$$

The maximum value of the grid reference current is obtained by adding all losses, the actual power of the load, and the contribution of PV power, which is stated as

$$I_{gp} = I_{Lp} + I_{loss} - I_{pv}. \quad (8)$$

To determine the instantaneous grid current, multiply deriving the synchronization signal by dividing the greatest value of the reference grid current by the PCC voltage. The VSC's gating pulses are activated when the current controller detects grid current, which is based on the standard grid current.

**B. Regulation of VSC in Islanded Mode**

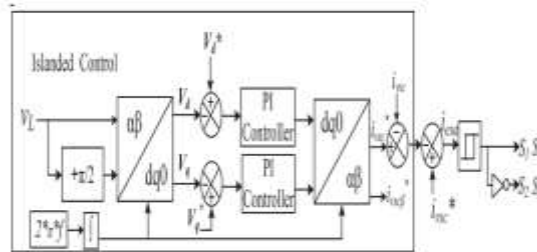


Fig. 5 Plan for controlling a single-phase voltage source converter

Figure 5 depicts the control technique for single-phase VSC using the  $\alpha\beta$  to dq transformation. By using in-phase, a perpendicular part of the load voltage, known as the  $\beta$  component, is generated. This component signifies the delay of one-fourth of a cycle in the load voltage. The voltage error for PI controllers is determined by comparing the generated contrast the dq voltage components with the conventional dq components. The VSC current's dq components are produced by the PI controller and then transformed into  $q\beta$  components. The formula for changing dq to  $q\beta$  and vice versa is:

$$\begin{bmatrix} v_{L\alpha} \\ v_{L\beta} \\ 0 \end{bmatrix} = \begin{bmatrix} \cos\omega t & -\sin\omega t & 0 \\ \sin\omega t & \cos\omega t & 0 \\ 0 & 0 & 1 \end{bmatrix} \begin{bmatrix} v_{Ld} \\ v_{Lq} \\ 0 \end{bmatrix} \quad (9)$$

$$\begin{bmatrix} i_{Ld} \\ i_{Lq} \\ 0 \end{bmatrix} = \begin{bmatrix} \cos\omega t & \sin\omega t & 0 \\ -\sin\omega t & \cos\omega t & 0 \\ 0 & 0 & 1 \end{bmatrix} \begin{bmatrix} i_{vsc\alpha} \\ i_{vsc\beta} \\ 0 \end{bmatrix}. \quad (10)$$

Generating single-phase VSC switching pulses requires comparing the observed VSC current with the in-phase component ( $i_{vsc\alpha}$ ).

**C. Battery Storage Administration**

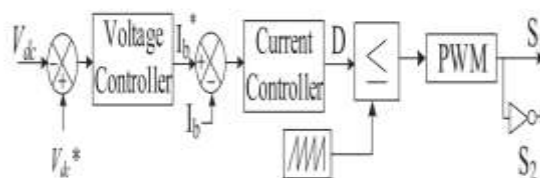


Fig.6 Battery Controller

The voltage between the reference and measured dc-links is used to regulate the amount of energy stored in the batteries. The procedure of sending this comparison to the PI processor in order to obtain a rough estimate of the battery reference current is illustrated in Figure 6. To compute pulses for the bidirectional converter, the comparison result between  $I_{batt\&}$  and the measured battery current ( $I_{batt}$ ) must be sent to the PI current controller.

$$D(n+1) = D(n) + k_{pi}\{I_{berr}(n+1) - I_{berr}(n)\} + k_{ii}I_{berr}(n+1) \quad (11)$$

$K_{pi}$  and  $k_{ii}$  represent the integral and relative gains of the PI controller are these.  $I_{berr}$  shows the incorrect battery current while  $D$  shows the duty ratio. In the event that the utility and PV sources are disabled, the DC link voltage will decrease. During the boost mode of the converter, transfers power from the battery to the DC-link to deliver power to certain applications, resulting in the battery being depleted. When photovoltaic electricity is available during a grid disruption, the voltage at the direct current link rises. The converter enables the flow of power from the DC-link to the battery and charges it by switching to buck mode. If a photovoltaic array experiences a failure, the battery is also controlled in the grid-connected setup. When the battery's SOC drops below a predetermined threshold ( $\leq 90\%$ ), the current controller starts injecting current. This happens when the cost of energy per unit is typically low. When neither the PV array nor the grid is accessible, the DC connection voltage drops, causing the battery to discharge and power the load.

#### D. PID Controller

A PID regulator, a fundamental subsidiary regulator, is commonly used as a control loop input device in modern control systems. It would be incorrect if the actual set point differed from the ideal set point and a deliberate cyclic variable. To reduce mistakes, the regulator adjusts the interaction using a controlled variable. The PID regulator calculation is sometimes called three-term control since it consists of three separate consistent parameters: P, I, and D. The features can be interpreted as follows: Here, I represents the total number of errors up to this point, P stands for the current error, and D is an estimate of future mistakes based on the current rate of change. To adjust the cycle using a control component, a weighted combination of force applied to a warming component, position of a control valve, or a damper is used. Without knowledge of the underlying interaction, a PID controller is universally regarded as the most effective regulator. Adjusting the three limitations in the PID regulator calculation can enable the use of specific interaction requirements to trigger the regulator's control function. The manipulated variable (MV) is collectively determined by the three adjusting terms in the PID control system. The combined value of the equivalent, necessary, and subordinate words influences the output of the PID regulator. The controller designers divide the Proportional, Integral, and Derivative modes into three separate structures or calculations for the regulator, represented by  $(b)$ . The regulator yield is represented by the symbol  $(b)$ . These terms pertain to interactive, non-intelligent, and parallel calculations. Some regulator manufacturers offer a setting feature in the regulator software that allows users to choose from various computation options. PID algorithms comprise:

##### 1) Interactive Algorithm

$$u(t) = K_c \left[ e(t) + \frac{1}{T_i} \int_0^t e(\tau) d\tau \right] * \left[ 1 + T_d \frac{d}{dt} e(t) \right]$$

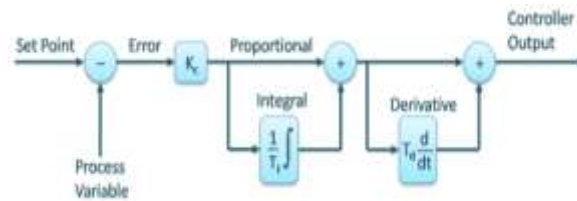
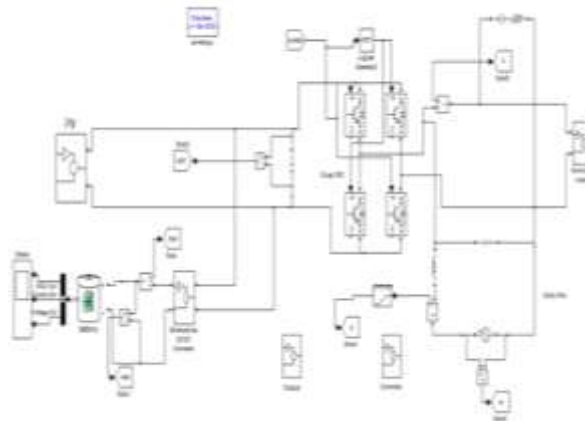


Fig.7 Algorithm with interactive features

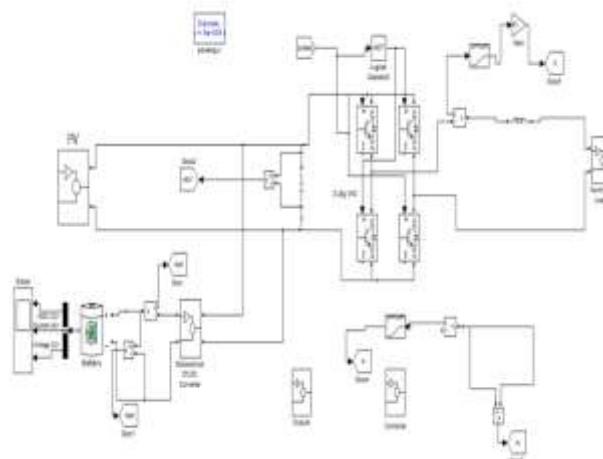
#### IV. ANALYSIS AND CONVERSATION

Initially, a PV-battery-based microgrid is developed using MATLAB/Simulink and a bidirectional converter to control the battery. The microgrid is then equipped with a step-adaptive filter that is adjustable. This chapter analyzes the microgrid's capacities in grid failure and recovery situations, focusing on reactive power compensation and improved dynamic responsiveness. The residential load at the point of common coupling consists of a nonlinear combination of resistance, inductance, and a diode bridge rectifier. The simulation is performed in MATLAB to analyze various operational circumstances. Abnormal grid conditions such as disruptions, voltage sag, harmonics in the PCC voltage, and voltage swell are considered in conjunction with changes in solar insolation. Various simulated scenarios are used to demonstrate the properties of the PV-battery system.

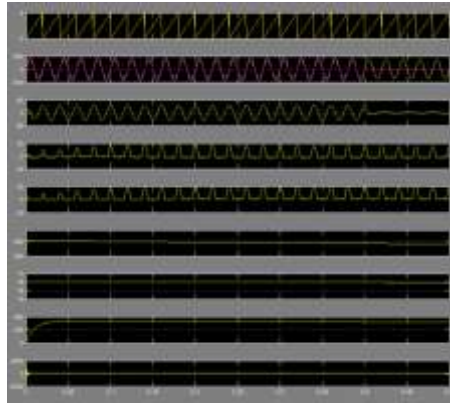
##### 1. SIMULATION MODEL AT SUDDEN RECOVERY OF UTILITY GRID



##### 2. SIMULATION MODEL AT DISAPPEARANCE OF UTILITY GRID

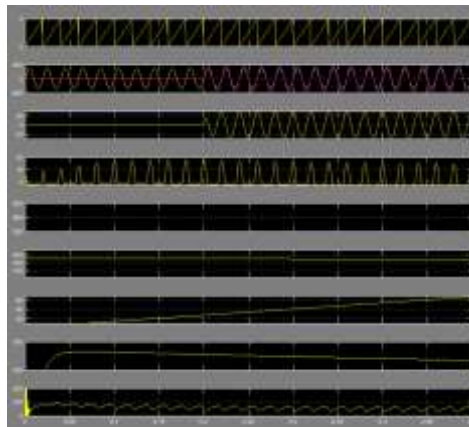


##### Performance at Disappearance of Utility



The previous picture shows how the microgrid reacts when the utility grid is not available. Under these circumstances, the phase angle difference steadily rises, causing the static switches to receive an OFF signal represented by "0" from the smooth transition algorithm. The battery is charged based on its current state of charge, and the battery voltage is kept within the specified range during islanded mode. The solar generator supplies energy for both immediate use and storage. During a grid failure, the distribution network disconnects from the microgrid, and the grid voltage's amplitude, angle, and frequency deviate from the set values. A bidirectional converter is used to boost the voltage from 240 V to 400 V. The BES's lowering of the second harmonic enhances the battery's longevity.

#### **Grid's Sudden Recovery Performance**



The above image shows the results of the modeling for the PV-battery multifunctional system in scenarios when the system is paid for by the utility company. Grid vs, along with  $v_L$ ,  $i_L$ ,  $V_{dc}$ ,  $V_{batt}$ ,  $V_{pv}$ , and  $I_{pv}$ , exhibit the outcomes. A connection between the utility and the VSC is established, the issue is resolved, and the SCADA Trip System is activated after 0.2 seconds. Electricity is being wired into the distribution network by VSC using adjustable step-based current regulation technology. There is no data in "is" or "vs" during the initial half-second. Upon configuration of the distribution network, vs and  $v_L$  have identical magnitudes, angles, and frequencies. In times of crisis, demand has little effect on energy use. At all times, the correct voltage levels are maintained for the battery and dc-link.

#### **CONCLUSION**

Incorporating a self-adjusting, step-based control algorithm and a single-phase, two-stage PV battery system, it was designed with a grid-interactive multifunctional architecture that can both feed power to the utility's single-phase alternating current system and deliver power in the event of a distribution network outage. Also, while PCC is operating in grid-interactive mode, this enhances its quality. Instructions for a tool that adapts to its environment was built to determine the maximum discharge current of the crucial component. Behavior, variations in photovoltaic irradiation, and adverse utility situations have all been investigated. The PV-battery system meets the IEEE-519 standard by removing the harmonic component from the utility and decreasing line and grid current

losses to less than 5%, despite the presence of a nonlinear load with a THD greater than or equal to 22.6% at the Point of Common Coupling .The PV grid-interactive system operates efficiently under both steady-state and dynamic circumstances.

## REFERENCES

- [1]. Ministry of New and Renewable Energy, Government of India, "Performance analysis of grid connected solar power projects comm. under Phase I of JNNSM, Jan.–Dec. 2014," 2015, pp. 1–4.
- [2]. A. Askarzadeh and L. Coelho, "A novel framework for optimization of a grid independent hybrid renewable energy system: A case study of Iran," *Solar Energy*, vol. 112, pp. 383–396, Feb. 2015.
- [3]. P. Kushwaha and C. Bhende, "Single-phase rooftop photovoltaic based grid-interactive electricity system," in *Proc. IEEE Annu. India Conf.*, 2016, pp. 1–6.
- [4]. N. Kim and B. Parkhideh, "Control and operating range analysis of an ACstacked PV inverter architecture integrated with a battery," *IEEE Trans. Power Electron.*, vol. 33, no. 12, pp. 10032–10037, Dec. 2018.
- [5]. H. Trabelsi, "MPPT controllers for PV array panel connected to Grid," in *Proc. 18th Int. Conf. Sci. Techn. Autom. Control Comput. Eng.*, 2017, pp. 505–510.
- [6]. M. Elgendy, B. Zahawi, and D. Atkinson, "Assessment of the incremental conductance maximum power point tracking algorithm," *IEEE Trans. Sustain. Energy*, vol. 4, no. 1, pp. 108–117, Jan. 2013.
- [7]. [7] R. John, S. Mohammed, and R. Zachariah, "Variable step size perturb and observe MPPT algorithm for standalone solar photovoltaic system," in *Proc. IEEE Intern. Conf. Intell. Techn. Control Optim. Signal Process.*, 2017, pp. 1–6.
- [8]. [8] S. Deshpande and N. Bashme, "A review of topologies of inverter for grid connected PV systems," *Innovations Power Adv. Comput. Technol.*, 2017, pp. 1–6.
- [9]. [9] K. Givaki, D. Chen, and L. Xu, "Current error based compensations for VSC current control in weak grid for wind farm applications," *IEEE Trans. Sustain. Energy*, vol. 10, no. 1, pp. 26–35, Jan. 2019.
- [10]. [10] C. Jain and B. Singh, "A SOGI-FLL based control algorithm for single phase grid interfaced multifunctional SPV under non-ideal distribution system," in *Proc. Annu. IEEE India Conf.*, 2014, pp. 1–6.
- [11]. [11] H. Li, Y. Huang, and J. Lu, "Reactive power compensation and DC link voltage control using fuzzy-PI on grid-connected PV system with D-STATCOM," in *Proc. IEEE PES Asia-Pacific Power Energy Eng. Conf.*, 2016, pp. 1240–1244.
- [12]. [12] S. Kumar and B. Singh, "A multipurpose PV system integrated to a threephase distribution system using an LWDF-based approach," *IEEE Trans. Power Electron.*, vol. 33, no. 1, pp. 739–748, Jan. 2018.
- [13]. [13] S. Kumar and B. Singh, "Implementation of high-precision quadrature control for single-stage SECS," *IEEE Trans. Ind. Inform.*, vol. 13, no. 5, pp. 2726–2734, Oct. 2017.
- [14]. [14] Z. Yao, L. Xiao, and Y. Yan, "Seamless transfer of single-phase grid interactive inverters between grid-connected and stand-alone modes," *IEEE Trans. Power Electron.*, vol. 25, no. 6, pp. 1597–1603, Jun. 2010.
- [15]. [15] B. Singh, A. Chandra, and K. Al-Haddad, *Power Quality: Problems and Mitigation Techniques*. India: Wiley-Blackwell, Jan. 2015.
- [16]. [16] IEEE Standard for Interconnection and Interoperability of Distributed Energy Resources with Associated Electric Power Systems Interfaces, IEEE Std 1547-2018 (Revision of IEEE Std 1547-2003), p. 1138, Apr. 2018.
- [17]. [17] C. Zhang, X. Zhao, X. Wang, X. Chai, Z. Zhang, and X. Guo, "A grid synchronization PLL method based on mixed second- and third-order generalized integrator for DC offset elimination and frequency adaptability," *IEEE J. Emerg. Sel. Topics Power Electron.*, vol. 6, no. 3, pp. 1517–1526, Sep. 2018.
- [18]. [18] C. Subramanian and R. Kanagaraj, "Rapid tracking of grid variables using prefiltered synchronous reference frame PLL," *IEEE Trans. Instrum. Measur.*, vol. 64, no. 7, pp. 1826–1836, Jul. 2015.
- [19]. [19] T. Youssef and O. Mohammed, "Adaptive SRF-PLL with reconfigurable controller for microgrid in grid-connected and stand-alone modes," in *Proc. IEEE Power Energy Soc. General Meeting*, 2013, pp. 1–5.
- [20]. [20] M. Ghartemani, S. Khajehoddin, P. Jain, and A. Bakhshai, "Problems of startup and phase jumps in PLL systems," *IEEE Trans. Power Electron.* vol. 27, no. 4, pp. 1830–1838, Apr. 2012.
- [21]. [21] R. Chilipi, N. Sayari, K. Hosani, M. Fasil, and A. Beig, "Third order sinusoidal integrator

- (TOSSI)- control algorithm for shunt active power filter under distorted and unbalanced voltage conditions,” *Int. J. Elect. Power Energy Syst.*, vol. 96, pp. 152–162, 2018.
- [22]. [22] D. Mlakić, S. Nikolovski, and H. Baghaee, “Hybrid method for islanding detection of distributed generators in LV distribution networks,” in *Proc. 18th IEEE Int. Conf. Smart Technol.*, 2019, pp. 1–6.
- [23]. [23] A. Abokhalil, A. Awan, and A. Al-Qawasmi, “Comparative study of passive and active islanding detection methods for PV grid-connected systems,” *MDPI*, vol. 10, pp. 1–15, May 2018.
- [24]. [24] H. Li, Z. Wu, and F. Lui, “A novel variable step size adaptive harmonic detecting algorithm applied to active power filter,” in *Proc. IEEE Int. Conf. Ind. Technol.*, 2016, pp. 574–578.